The effect of acute intraocular pressure elevation on peripapillary retinal thickness, retinal nerve fiber layer thickness and retardance

Brad Fortune[1], **Hongli Yang**[1,B], **Nicholas G. Strouthidis**[1,B], **Grant A. Cull**[1], **Jonathan L. Grimm**[1,B], **J. Crawford Downs**[1,C], and **Claude F. Burgoyne**[1,B]

[1]Discoveries in Sight Research Laboratories, Devers Eye Institute, Legacy Health System, Portland, OR, USA

[B]Optic Nerve Head Research Laboratory

[C]Ocular Biomechanics Laboratory

Abstract

Purpose—To determine whether acutely elevated intraocular pressure (IOP) alters peripapillary retinal thickness, retinal nerve fiber layer thickness (RNFLT) or retardance.

Methods—Nine adult non-human primates were studied under isoflurane anesthesia. Retinal and RNFL thicknesses were measured by spectral domain optical coherence tomography 30 min after IOP was set to 10 mmHg and 60 min after IOP was set to 45 mmHg. RNFL retardance was measured by scanning laser polarimetry in 10 min intervals for 30 min while IOP was 10 mmHg, then for 60 min while IOP was 45 mmHg, then for another 30 min after IOP was returned to 10 mmHg.

Results—RNFLT measured 1120 μm from the ONH center decreased from 118.1 ± 9.3 μm at an IOP of 10 mmHg to 116.5 ± 8.4 μm at 45 mmHg, or by $1.4 \pm 1.8\%$ ($p<0.0001$). There was a significant interaction between IOP and eccentricity ($p=0.0006$). Within 800 μm of the ONH center, the RNFL was $4.9 \pm 3.4\%$ thinner 60 min after IOP elevation to 45 mmHg ($p<0.001$), but unchanged for larger eccentricities. The same pattern was observed for retinal thickness, with $1.1 \pm 0.8\%$ thinning overall at 45 mmHg ($p<0.0001$), and a significant effect of eccentricity ($p<0.0001$) whereby the retina was $4.8 \pm 1.2\%$ thinner ($p<0.001$) within 800 μm, but unchanged beyond that. Retardance increased by a maximum of $2.2 \pm 1.1\%$ 60 min after IOP was increased to 45 mmHg ($p=0.0031$).

Conclusions—The effects of acute IOP elevation on retinal thickness, RNFL thickness and retardance were minor, limited to the immediate ONH surround and unlikely to have meaningful clinical impact.

Keywords

retinal ganglion cell; retinal nerve fiber layer; scanning laser polarimetry; optical coherence tomography; intraocular pressure

Corresponding Author: Brad Fortune, OD, PhD, Associate Scientist, Devers Eye Institute, 1225 NE Second Avenue, Portland, OR 97232, Phone: 503-413-1198, Fax: 503-413-5179, Email: bfortune@deverseye.org.

Introduction

Retinal nerve fiber layer (RNFL) defects are a structural manifestation of the damage caused by glaucoma[1] and frequently precede the development of glaucomatous vision loss.[2-6] Therefore, assessment of the RNFL is recognized as an important procedure in the routine clinical care of all glaucoma patients and suspects. However, detecting such defects during their earliest stages can prove difficult by clinical fundoscopy or photography,[7] so it is hoped that advancements in imaging techniques such as optical coherence tomography (OCT)[8-11] and scanning laser polarimetry (SLP)[12,13] will improve clinical capabilities for detecting early glaucomatous RNFL damage and its progression.[14-18]

RNFL assessment by OCT[8-11] capitalizes on the fact that the RNFL produces relatively strong reflectance of the imaging source whereas SLP[12,13,19] detects the relative phase retardance of a polarized light source induced by the birefringent properties of the RNFL. Both of these optical characteristics are thought to be due to the long, thin cylindrical shape and parallel orientation of the internal cytoskeleton - principally the microtubules - within retinal ganglion cell (RGC) axons of the RNFL.[20-26]

Acute and chronic intraocular pressure (IOP) elevation are known to cause cytoskeletal abnormalities and disrupt axonal transport resulting in organelle accumulation and axonal swelling near the lamina cribrosa.[27-34] It is therefore possible that RNFL measurements such as those made using OCT or SLP could be affected by elevated IOP through such secondary effects, or perhaps directly by compression. It is important to differentiate the relatively acute IOP-related effects from chronic disease-related changes in order to arrive at accurate clinical diagnoses and to reveal potentially meaningful pathophysiological information or susceptibility. Currently, it is unknown whether peripapillary RNFL thickness or retardance are affected by the acute level of IOP. Therefore, the purpose of this study was to determine whether acute IOP elevation affects peripapillary RNFL thickness or retardance measurements in normal non-human primate (NHP) eyes.

Methods

Subjects

In total, nine adult female rhesus macaque monkeys (*Macaca mulatta*) were included in this study, five in the retinal and RNFL thickness experiment and four in the retardance experiment. Table 1 lists the age and weight of each animal, as well as the experiment to which each was assigned. All experimental methods and animal care procedures adhered to the Association for Research in Vision and Ophthalmology's Statement for the Use of Animals in Ophthalmic and Vision Research and were approved by the local Institutional Animal Care and Use Committee (IACUC).

Anesthesia

All experimental procedures began with induction of general anesthesia using ketamine (15 mg/kg IM) and midazolam (0.2 mg/kg IM). A single subcutaneous injection of atropine sulphate (0.05 mg/kg) was also administered. Animals were then intubated and breathed 100% oxygen and isoflurane gas (1-2%) to maintain anesthesia for the duration of the imaging session. Heart rate and arterial oxyhemoglobin saturation were monitored continuously (Propaq Encore model 206EL, Protocol Systems, Inc., Beaverton, OR) and maintained above 75 min^{-1} and 95%, respectively. Body temperature was maintained with a warm-water heating pad set at 37°C. Blood pressure was measured approximately every 10 minutes (NIBP system 7100, Advanced Medical Instruments, Inc., Broken Arrow, OK) and maintained above a mean arterial pressure of 75 mmHg with IV lactated Ringer's delivered if necessary (10 ml/kg/hr).

If mean arterial pressure decreased below 75 mmHg despite IV fluid administration, the imaging session was discontinued and the animal recovered immediately.

Manometric IOP control

after application of topical anesthesia (0.5% proparacaine) the anterior chamber was cannulated by insertion of a 27-guage needle through the peripheral cornea. The needle was connected via polyethylene tubing to an adjustable-height reservoir of sterile balanced salt solution (BSS, Alcon Laboratories, Inc.). The height of the reservoir was pre-calibrated in 5 mmHg increments using a pressure transducer (MX860; Medex, Inc., Carlsbad CA). OCT and SLP scans were obtained with IOP set to 10 mmHg (baseline) and 45 mmHg (acutely elevated IOP) as outlined below for each experiment. At the end of the imaging session the needle was removed and a broad-spectrum topical antibiotic ointment was applied.

Experiment 1; data acquisition

RNFL and total retinal thickness measurements were obtained by spectral-domain optical coherence tomography (SD-OCT) using a Spectralis™ OCT instrument (Heidelberg Engineering, GmbH, Heidelberg, Germany). The optical resolution of the instrument is ~7 μm axially and ~14 μm transversely. The depth of each A-scan is 1.8 mm and consists of 512 pixels providing a digital depth sampling of 3.5 μm per pixel. Each B-scan spans 15 degrees and consists of 768 A-scans providing a digital transverse sampling of 5 μm per pixel (in an emmetropic human eye with average axial length). For this experiment, B-scans were arranged in a radial pattern centered on the optic disk. The radial pattern consisted of 48 B-scans for one subset of animals (n=2) and 80 B-scans for the others (n=3, see Table 1). In the latter cases, only 40 of the 80 B-scans were used (i.e. manual segmentation was performed on every second scan beginning with the vertical scan). A real-time eye tracking system measures eye movements and provides feedback to the SD-OCT scanning system in order to stabilize the retinal position of each B-scan. This allows sweep averaging to be employed for reduction of speckle noise. For this experiment, nine sweeps were averaged for each B-scan.

OCT 'raw' data were then exported from the Spectralis instrument in order to complete manual segmentation of B-scan features using custom-built, "Multiview" 3-D visualization and delineation software that is based on the Visualization Toolkit (VTK, Clifton Park, NY). Figure 1 provides an example of the segmentation process. The B-scan shown in Fig. 1A represents the vertical section from a radial pattern with 80 b-scans total. It was acquired 30 minutes after IOP was set to 10 mmHg. The colored marks were positioned manually within the software to begin segmentation of the various B-scan features delineated in this study. As the marks of each feature class are placed, the Bézier curves shown in corresponding colors are fitted in real time. The position of each mark is adjusted manually so that the Bézier curve accurately delineates the intended feature. The initial segmentations were performed by a trained technician, then one of the investigators (NS) reviewed the segmentations for fine tuning and/ or corrections. Both technician and investigator were masked to the IOP condition of all scans.

The green marks and green Bézier curve represent the border between the vitreous and the inner limiting membrane (ILM), which was defined as the anterior RNFL border for the purposes of this study. The blue marks and blue Bézier curves on either side of the ONH represent the posterior RNFL border. The orange marks and orange Bézier curves represent the posterior aspect of the retinal pigment epithelium-Bruch's membrane (RPE-BM) complex. The pair of red marks on each side of the ONH defines the neural canal opening (NCO).[35] Fig. 1B shows the full set of marks, for these four segmentation classes and all 40 radial B-scans, overlaid onto the infrared reflectance image acquired for this eye at the time of the OCT scan. In Fig. 1D, the corresponding Bézier curves are shown above the reflectance image from a different perspective.

The schematic shown in Fig. 1C demonstrates the method used to derive RNFL thickness values from the B-scan segmentation results. First, the Bézier curve defining the posterior RNFL surface is sampled in 10-μm intervals. From each of these sampled points along the posterior RNFL border, a vector is cast within the plane of the B-scan toward the segmented anterior RNFL border to determine the minimum distance between them. In this schematic, the vector solution for each sampled point is shown as a purple-colored line. A radius is also calculated for each sampled point along the posterior RNFL border. The radius is the distance to the centroid of an ellipse, which itself is fitted to the family of segmented NCO points.[35] In Figure 1C, three of the RNFL thickness vectors are shown as black arrows pointing toward the anterior RNFL border. Each of these three sample points also has a grey arrow pointing toward the plane of the NCO ellipse where its intersection defines the coordinate used to determine the radius. This coordinate system enabled alignment of paired SD-OCT volumes (baseline and elevated IOP time points) by translation to a commonly defined origin (the NCO centroid) and by rotation to commonly defined radial axes (the major and minor axes of the NCO ellipse). It thus helped minimize error due to minor differences in scan pattern placement between time points (e.g. Figs. 1E and 1F show alignment) and enabled derivation of difference maps for topographical visualization of results (e.g. Fig. 1G).

Total retinal thickness values were derived in the same manner except that the Bézier curve defining the posterior aspect of the RPE-BM complex was sampled rather than the posterior RNFL border. Similar topographical maps were used to visualize results (e.g. Figs. 1H-J). These continuous maps were constructed by interpolating values between each radial B-scan.

Experiment 1 design and analysis; effect of acute IOP elevation on RNFL thickness and total retinal thickness

The experiment was performed bilaterally during a single session for each of the five animals (see Table 1). Both anterior chambers were cannulated and IOP was set to 10 mmHg. OCT scans were obtained in each eye after a 30-minute stabilization period. The scan obtained after 30 minutes of IOP set at 10 mmHg was defined as the baseline against which the scans obtained after acutely elevated IOP were compared. Additionally, in 6 eyes of 3 animals (ID# 5, 6 and 7, Table 1), we also obtained a scan 10 minutes after IOP had been set to 10 mmHg; this scan was paired with the 30 minutes time point at an IOP of 10 mmHg to serve as a control for evaluation of inter-scan repeatability in the absence of any IOP change. Following the scan obtained at 30 minutes with IOP set to 10 mmHg, in all 10 eyes, IOP was then raised to 30 mmHg for 30 minutes, at which time OCT scans were repeated. IOP was then raised further to 45 mmHg for an additional 60 minutes after which OCT scans were repeated again. For the purposes of this study, only the data for the IOP = 45 mmHg condition (60 minutes of IOP = 45 mmHg, but 90 minutes of total IOP elevation) were compared with the stabilized baseline of 30 minutes at an IOP of 10 mmHg.

RNFL thickness values for control and elevated IOP conditions were compared using repeated measures analysis of variance (RM-ANOVA, Prism v4, GraphPad Software, Inc). Analysis was performed on data for a fixed peripapillary eccentricity chosen to match the location of SLP retardance measurements, as well as on the sum of all thickness samples within each B-scan section. Two-way RM-ANOVA was applied to determine whether there were significant interactions between acute IOP elevation and polar angle or between acute IOP elevation and eccentricity. Analysis of total retinal thickness data was performed in the same manner.

Experiment 2; data acquisition

RNFL retardance measurements were obtained by SLP using a GDxVCC instrument (Carl Zeiss Meditec, Inc., Dublin, CA). The instrument compensates for the effects of anterior segment birefringence to more accurately determine RNFL retardance.[13,36] Thus, the axis and

magnitude of anterior segment birefringence are derived from uncompensated images prior to initial baseline RNFL scans, then used to compensate all subsequent RNFL scans. A bite-bar, which rotates in three axes, was used to properly align the head and eye, and auto-refraction is used for each scan. Three RNFL scans were averaged for each eye at each time point.

The GDxVCC instrument detects the relative phase retardance of a cross-polarized laser imaging source after a double pass through the tissue sample, assumes that RNFL thickness is linearly related to retardance, then calculates and reports an estimate of RNFL "thickness" using a linear conversion factor of 0.67 nm/μm[12,37]. Values of RNFL thickness were exported for the small peripapillary locus (the SLP instrument's default), then divided by the conversion factor and reported here as retardance values. The exported data consist of 64 samples along a peripapillary locus beginning on the temporal side of the ONH, proceeding around the superior, nasal, inferior aspects of the ONH and completing a circle at the temporal location, thus representing a profile commonly referred to as a "TSNIT" curve. Each of the values in the TSNIT curve is an average from an 8-pixel wide band centered on the optic disc.[37] The inner and outer limits of the band are 27 and 35 pixels from the center of the optic disc, so the center of the band has a radius of 31 pixels.[37] This corresponds to a scan angle with a radius of 6.1 degrees,[37] which translates to about 1120 μm on the macaque retina (assuming an emmetropic eye with average axial length of 19 mm).[38-40]

Experiment 2 design and analysis; effect of acute IOP elevation on RNFL retardance

Only one eye was imaged by SLP during a given session in order to maintain optimal alignment and increase temporal resolution. Initially, a set of 3 SLP scans was obtained prior to anterior chamber cannulation, thereafter another set of 3 SLP scans was obtained at each time point. Time points were separated by 10-minute intervals. There were three time points during the baseline stabilization period after cannulation during which IOP was set to 10 mmHg. IOP was then raised to 45 mmHg and a set of 3 SLP scans was obtained every 10 minutes for 1 hour (6 time points). IOP was then lowered back to 10 mmHg and followed for a 30-minute recovery period, again with a set of 3 SLP scans averaged at each of three recovery time points.

Repeated-Measures ANOVA was applied to assess the main effect of acute IOP elevation using the raw retardance samples from the peripapillary (TSNIT) profile for each eye and time point. Two-way RM-ANOVA was also applied to determine whether there was any significant interaction between subject and acute IOP elevation.

Results

After 60 minutes of acute IOP elevation from 10 to 45 mmHg, the most readily apparent changes revealed by SD-OCT were in the architecture of the ONH as previously reported (Burgoyne CF, et al. *IOVS* 2008;49:ARVO E-Abstract 3655). Figure 2 shows a horizontal section through the center of the ONH of one eye. The B-scan in the top panel was acquired 30 minutes after IOP was set to 10 mmHg. The B-scan in the bottom panel was acquired after 60 minutes of IOP set to 45 mmHg. In each panel, the dashed white line connects the points 15° on either side of the ONH at the posterior aspect of the RPE-BM complex (i.e. the two peripheral points of the RPE-BM) and serves as a reference line. Figure 2 shows that the ONH surface exhibited posterior displacement relative to the reference line when IOP was elevated to 45 mmHg for 60 minutes (arrowhead). Changes in the shape of the peripapillary connective tissues were also consistently observed, such as posterior deformation of the RPE-BM complex immediately adjacent to the ONH (arrows). The depth of the NCO centroid relative to the plane defined by the peripheral RPE-BM complex at the outer edge of the scan increased by 41.2 ± 17.1 μm (range 18 to 71 μm, $p<0.0001$), suggesting that deformation of the ONH and peripapillary connective tissues during acutely elevated IOP includes posterior displacement. For the 6 eyes in which control data were available, the average difference in this dimension

between 10 and 30 minutes of IOP set to 10 mmHg was 0.7 ± 18.1 μm ($p = 0.93$). Though these ONH changes are relevant, the focus of this study is the peripapillary retina, therefore further details of ONH response to acute IOP elevation will be the subject of future reports.

Peripapillary retinal and RNFL thicknesses were represented by topographic pseudo-color maps for visualizing results as shown in Fig. 1. Panels 1E and 1F represent RNFL thickness 30 minutes after IOP was set to 10 mmHg, and 60 minutes after IOP was set to 45 mmHg, respectively. Panels 1H and 1I represent total retinal thickness in the same eye for the same two conditions. The posterior RNFL border was frequently difficult to discern near the ONH as reflected by the gap surrounding the NCO points in each of the RNFL topographic maps (1E and 1F, see also blue-colored segmentation line in 1A). However, RNFL thickness values were present for all sections in all eyes for radii of 1400 μm and longer. Note that 1400 μm refers to the linear dimension converted from angular subtense by the Spectralis instrument assuming an emmetropic human eye with average axial length. Our calculations estimate that this dimension actually corresponds to ~1120 μm in the NHP eye with a 19 mm axial length. [38-40] The effect of acute IOP elevation on RNFL thickness was analyzed first for this particular eccentricity because it matches the standard SLP peripapillary measurement locus.

RNFL thickness at this eccentricity was 118.1 ± 9.3 μm 30 minutes after IOP was set to 10 mmHg (n=10 eyes, 5 animals). Then 60 minutes after IOP was increased to 45 mmHg, the average RNFL thickness at this eccentricity was 116.5 ± 8.4 μm, or 1.4% ($\pm 1.8\%$) thinner ($p<0.0001$, RM-ANOVA). The effect of acute IOP elevation was thus small in magnitude but statistically significant because it was consistent across eyes and peripapillary (TSNIT) locations. The latter two variables accounted for nearly all of the RNFL thickness variability (15%, $p<0.0001$ and 83%, $p<0.0001$, respectively). There was no significant interaction between acute IOP elevation and radial peripapillary (TSNIT) location (i.e. polar angle, $p=0.80$), however it is possible that the 1.4% thinning represents constriction of the retinal blood vessels within the RNFL, as Fig. 3 shows that the effect on average manifests predominantly at the superior and inferior positions where retinal vessels make a substantial contribution to the cross-sectional area of the RNFL.[41]

When the RNFL thickness analysis included data from all eccentricities a similarly small degree of thinning was found overall ($2.7\% \pm 3.6\%$, $p<0.0001$, two-way RM-ANOVA). However there was a significant interaction between elevated IOP and retinal eccentricity ($p=0.0006$) such that the effect was larger closest to the ONH and diminished with increasing distance from the NCO (Fig. 4). Within 800 μm of the NCO, the RNFL was $4.9\% \pm 3.4\%$ thinner after 60 minutes of IOP elevation to 45 mmHg ($p<0.001$), whereas there was no significant change for eccentricities larger than 800 μm (analyzed in eccentricity bins of 250 μm, Fig. 4). Note that the eccentricity values represent the linear dimension converted from angular subtense by the Spectralis instrument for human eyes then scaled by 0.8 for the NHP eye with a 19 mm axial length. For the 6 eyes in which control data were available, overall RNFL thickness was $1.2 \pm 1.0\%$ thicker 30 minutes after IOP was set to 10 mmHg as compared with 10 minutes of IOP set to 10 mmHg ($p = 0.04$). Thus, the effect of acute IOP elevation, though very small, was approximately twice the magnitude of inter-scan variability of the control condition.

Total retinal thickness at the "1400 μm" eccentricity (~1120 μm in the NHP eye) was 332.7 ± 13.9 μm after 30 minutes of IOP set to 10 mmHg (n=10 eyes, 5 animals, Fig. 5). After 60 minutes of IOP set to 45 mmHg, total retinal thickness was 333.5 ± 12.8 μm. At this eccentricity, the average change in retinal thickness between IOP levels was a small but significant increase of $0.3\% \pm 1.0\%$ ($p=0.0006$). There was no significant interaction between IOP level and radial (TSNIT) position ($p=0.99$, Fig. 5).

When data for all eccentricities were included in the analysis of total retinal thickness, a minor degree of thinning was found overall ($1.1\% \pm 0.8\%$, $p<0.0001$, two-way RM-ANOVA). However, as found for RNFL thickness, there was a significant interaction between elevated IOP and retinal eccentricity ($p<0.0001$) whereby the effect of acutely elevated IOP was only significant within 800 μm from the center of the ONH (Fig. 6). The retina was $4.8\% \pm 1.2\%$ thinner after 60 minutes of IOP elevation to 45 mmHg ($p<0.001$) within 800 μm of the NCO, whereas there was no significant change for eccentricities larger than 800 μm (analyzed in eccentricity bins of 200 μm, Fig. 6). For the 6 eyes in which control data were available, total retinal thickness was $1.0 \pm 0.6\%$ thicker 30 minutes after IOP was set to 10 mmHg as compared with 10 minutes of IOP set to 10 mmHg ($p = 0.01$). Thus, the effect of acute IOP elevation on retinal thickness was small and approximately equal to the magnitude of inter-scan variability of the control condition. In contrast to the effect of acute IOP elevation, however, there was no significant interaction between eccentricity and time for the control comparison ($p = 0.78$), suggesting that the small degree of retinal thinning near the ONH after acute IOP elevation is a real effect.

Figure 7 shows the result of acute IOP elevation on RNFL retardance. During the 30-minute baseline period when IOP was 10 mmHg, the average peripapillary RNFL retardance was 36.1 nm (n= 8 eyes, 4 monkeys). This increased to an average of 36.6 nm during the 60-minute period when IOP was elevated to 45 mmHg ($p = 0.0031$, RM-ANOVA). This small but statistically significant increase is more clearly visualized in Fig. 7B, where retardance values are normalized relative to the average baseline value for each eye. The average increase across the 60-minute period of IOP elevation was 1.5%; the peak effect, which occurred at the final 60-minute time point, was $2.2\% \pm 1.1\%$. RNFL retardance varied across subjects as expected ($p < 0.0001$), and there was a high correlation between the two eyes of each subject ($p < 0.0001$), however, there was no significant interaction between the effects of acute IOP elevation and subject ($p = 0.61$; with eyes matched for each subject).

Discussion

The results of this study show that acute IOP elevation from 10 to 45 mmHg in healthy NHP eyes had only minor effects on peripapillary retinal thickness, RNFL thickness and retardance. Though the effects on ONH architecture and immediately adjacent structures could be relevant to glaucoma pathophysiology, the minor effects observed here for the peripapillary retina and RNFL are not likely to have meaningful impact on clinical practice. Indeed, the effects were so small that one could interpret the results to mean that the acute IOP level is not important for clinical measurements of the peripapillary retina and RNFL. That is, when patients present with elevated IOP at the time of clinical imaging, the outcome is likely to represent their chronic status of the peripapillary retina and RNFL rather than being due to any direct effect of acutely elevated IOP.

The small decrease observed for both retinal and RNFL thickness 60 minutes after IOP was elevated to 45 mmHg occurred only in the immediate peripapillary region, where the connective tissue architecture was also observed to change (Fig. 2). Thus, although the results for larger distances from the center of the ONH suggest that neither the retina nor the RNFL are mechanically compressible, the results nearer to the ONH suggest that there are potentially important regional differences in response to elevated IOP. For example, it is possible that the changes in peripapillary and ONH connective tissue architecture cause the immediate peripapillary retina and RNFL to stretch and thus become marginally thinner. Previous studies have demonstrated ONH surface height and conformational changes in response to acute IOP changes in both NHP[39,42-44] and human eyes[45,46] using other imaging techniques; OCT may now also enable study of effects beneath the ONH surface. Collectively, these changes within and immediately adjacent to the ONH may represent important mechanisms of RGC injury in

glaucoma, though any such inference is drawn on the basis of acute IOP elevation and therefore requires caution.

In a previous study using OCT, Aydin et al[47] found that the RNFL became thicker in glaucoma patients 6-12 months after surgical reduction of IOP. However, two similar studies reported that there was no significant change in RNFL thickness after surgical or medical IOP reduction in glaucoma patients.[48,49] Though the results of the present study are based on acute IOP elevation in healthy NHP eyes rather than longer-term follow-up after IOP lowering treatment of glaucoma patients, they do suggest one possibility for the discrepancy among those other studies. The initial study by Aydin et al used a prototype OCT system, whereas the other two recent studies used a commercial Stratus OCT instrument. It is possible that the average eccentricity was closer to the ONH for the Aydin et al study than for the others, even though all three reported using an approximately 1.7 mm radius for the circumpapillary scan. For example, the two studies reporting no change in RNFL thickness may have included a larger number of subjects with axial myopia, for whom the circumpapillary scan radius would have been effectively larger. In any case, the results of the present study suggest that analysis of more than a single peripapillary eccentricity could be beneficial to the study of both acute and chronic effects of IOP. Further, the present results suggest that if a single peripapillary circular sample is used to estimate RNFL thickness, it should be sufficiently distant from the ONH center to minimize effects of ambient IOP level. Most current systems sampling at a single eccentricity meet this criterion.

In contrast to the minor degree of retinal and RNFL *thinning* observed after acute IOP elevation, RNFL retardance actually *increased,* though by a similarly small percentage. Two minutes after a 45-second period of acute IOP elevation to 100 mmHg in human eyes, Iester et al also observed a 0.3% increase in retardance, a similarly small change that was not statistically significant in their study.[50] Though acute IOP elevation is known to alter axonal cytoskeletal components,[27-29,33,34] and that these components are the source of RNFL retardance measured by SLP,[20-26] it is unlikely that the acute retardance changes observed in this study represent acute cytoskeletal changes. RNFL retardance changes in this study occurred within minutes (Fig. 7) and were stable during the period of elevated IOP. Cytoskeletal changes are likely to a longer duration to manifest[34] and would likely result in progressively altered retardance.[24,26] An alternative explanation might be that the conformational changes of the peripapillary retina noted during acute IOP elevation (e.g. Fig. 2) cause the SLP scan path through the RNFL (and retina) to increase slightly and perhaps thus encounter a proportionally greater number of cytoskeletal elements. In the absence of any change in RNFL thickness, the increased path length would vary inversely with the cosine of the increased angle of incidence at the ILM. By this model the observed 1.4% retardance increase would require an approximately 10-degree change to have occurred in the angle of incidence between the scanning beam and RNFL. This angle is more than a factor of two larger than what was observed in most eyes including the example shown in Fig. 2, which is consistent with the average posterior displacement of the NCO being only 41 μm. Thus it is unlikely that this simple conformational model offers a complete explanation of the small change in retardance observed during acutely elevated IOP.

Though we did not measure axial length in this study, previous studies have shown that axial length measured by conventional A-scan ultrasonography (thus presumably close to or along the optical axis of the eye) does not change with acute IOP elevation to either 30 or 45 mm Hg.[39] The results of this study, and previous studies by our group (Burgoyne CF, et al. *IOVS* 2008;49:ARVO E-Abstract 3655) and others[39,42-44] suggest that surface height changes (in eyes where they occur at all) are limited to the ONH and immediate peripapillary retina, and would therefore not influence the conventional A-scan ultrasound measurement made close to the optical axis because deformations are localized to the ONH and do not involve the entire

scleral shell of the eye. Lastly, there were no corneal opacities or edema observed during any of the present experiments.

In summary, this study demonstrates that acute IOP elevation from 10 to 45 mmHg for 60 minutes in healthy NHP eyes resulted in only minor changes to peripapillary retinal thickness, RNFL thickness and retardance measurements. This suggests that changes in these parameters observed clinically during longitudinal follow-up of glaucoma patients represent true pathological changes due to chronic disease effects rather than artifactual variation due to the acute IOP level at the time of imaging. In this regard these parameters may be a more robust clinical measure of structural integrity than is ONH surface height, insofar as the latter is known to vary with acute IOP level.[39,42-46] An important caveat and limitation of this study is that it was not performed on glaucomatous nor human eyes and it is possible that human and/or unhealthy axons might respond to acute IOP changes differently than that reported here.

Acknowledgements

References

1. Hoyt WF, Frisen L, Newman NM. Fundoscopy of nerve fiber layer defects in glaucoma. Invest Ophthalmol 1973;12:814–29. [PubMed: 4752920]

2. Quigley HA, Enger C, Katz J, Sommer A, Scott R, Gilbert D. Risk factors for the development of glaucomatous visual field loss in ocular hypertension. Arch Ophthalmol 1994;112:644–9. [PubMed: 8185522]

3. Quigley HA, Katz J, Derick RJ, Gilbert D, Sommer A. An evaluation of optic disc and nerve fiber layer examinations in monitoring progression of early glaucoma damage. Ophthalmology 1992;99:19–28. [PubMed: 1741133]

4. Sommer A, Katz J, Quigley HA, Miller NR, Robin AL, Richter RC, Witt KA. Clinically detectable nerve fiber atrophy precedes the onset of glaucomatous field loss. Arch Ophthalmol 1991;109:77–83. [PubMed: 1987954]

5. Mohammadi K, Bowd C, Weinreb RN, Medeiros FA, Sample PA, Zangwill LM. Retinal nerve fiber layer thickness measurements with scanning laser polarimetry predict glaucomatous visual field loss. Am J Ophthalmol 2004;138:592–601. [PubMed: 15488786]

6. Lalezary M, Medeiros FA, Weinreb RN, Bowd C, Sample PA, Tavares IM, Tafreshi A, Zangwill LM. Baseline optical coherence tomography predicts the development of glaucomatous change in glaucoma suspects. Am J Ophthalmol 2006;142:576–82. [PubMed: 17011848]

7. Quigley HA. Examination of the retinal nerve fiber layer in the recognition of early glaucoma damage. Trans Am Ophthalmol Soc 1986;84:920–66. [PubMed: 3109098]

8. Huang D, Swanson EA, Lin CP, Schuman JS, Stinson WG, Chang W, Hee MR, Flotte T, Gregory K, Puliafito CA, et al. Optical coherence tomography. Science 1991;254:1178–81. [PubMed: 1957169]

9. Schuman JS, Hee MR, Puliafito CA, Wong C, Pedut-Kloizman T, Lin CP, Hertzmark E, Izatt JA, Swanson EA, Fujimoto JG. Quantification of nerve fiber layer thickness in normal and glaucomatous eyes using optical coherence tomography. Arch Ophthalmol 1995;113:586–96. [PubMed: 7748128]

10. Wollstein G, Paunescu LA, Ko TH, Fujimoto JG, Kowalevicz A, Hartl I, Beaton S, Ishikawa H, Mattox C, Singh O, Duker J, Drexler W, Schuman JS. Ultrahigh-resolution optical coherence tomography in glaucoma. Ophthalmology 2005;112:229–37. [PubMed: 15691556]

11. Skaf M, Bernardes AB, Cardillo JA, Costa RA, Melo LA Jr. Castro JC, Varma R. Retinal nerve fibre layer thickness profile in normal eyes using third-generation optical coherence tomography. Eye 2006;20:431–9. [PubMed: 16052259]

12. Weinreb RN, Dreher AW, Coleman A, Quigley H, Shaw B, Reiter K. Histopathologic validation of Fourier-ellipsometry measurements of retinal nerve fiber layer thickness. Arch Ophthalmol 1990;108:557–60. [PubMed: 2322159]

13. Weinreb RN, Bowd C, Zangwill LM. Scanning laser polarimetry in monkey eyes using variable corneal polarization compensation. J Glaucoma 2002;11:378–84. [PubMed: 12362075]

14. Schuman JS, Pedut-Kloizman T, Hertzmark E, Hee MR, Wilkins JR, Coker JG, Puliafito CA, Fujimoto JG, Swanson EA. Reproducibility of nerve fiber layer thickness measurements using optical coherence tomography. Ophthalmology 1996;103:1889–98. [PubMed: 8942887]

15. Stein DM, Wollstein G, Schuman JS. Imaging in glaucoma. Ophthalmol Clin North Am 2004;17:33–52. [PubMed: 15102512]

16. Medeiros FA, Zangwill LM, Bowd C, Mohammadi K, Weinreb RN. Comparison of scanning laser polarimetry using variable corneal compensation and retinal nerve fiber layer photography for detection of glaucoma. Arch Ophthalmol 2004;122:698–704. [PubMed: 15136317]

17. Wollstein G, Schuman JS, Price LL, Aydin A, Stark PC, Hertzmark E, Lai E, Ishikawa H, Mattox C, Fujimoto JG, Paunescu LA. Optical coherence tomography longitudinal evaluation of retinal nerve fiber layer thickness in glaucoma. Arch Ophthalmol 2005;123:464–70. [PubMed: 15824218]

18. Zangwill LM, Bowd C. Retinal nerve fiber layer analysis in the diagnosis of glaucoma. Curr Opin Ophthalmol 2006;17:120–31. [PubMed: 16552246]

19. Dreher, AW.; Reiter, K.; Weinreb, RN. Spatially resolved birefringence of the retinal nerve fiber layer assessed with a retinal laser ellipsometer. 1992.

20. Zhou Q, Knighton RW. Light scattering and form birefringence of parallel cylindrical arrays that represent cellular organelles of the retinal nerve fiber layer. Applied Optics 1997;36:2273–2285. [PubMed: 18253203]

21. Knighton RW, Huang XR. Visible and near-infrared imaging of the nerve fiber layer of the isolated rat retina. J Glaucoma 1999;8:31–7. [PubMed: 10084272]

22. Knighton RW, Huang XR. Directional and spectral reflectance of the rat retinal nerve fiber layer. Invest Ophthalmol Vis Sci 1999;40:639–47. [PubMed: 10067967]

23. Huang XR, Knighton RW. Linear birefringence of the retinal nerve fiber layer measured in vitro with a multispectral imaging micropolarimeter. J Biomed Opt 2002;7:199–204. [PubMed: 11966304]

24. Huang XR, Knighton RW. Microtubules contribute to the birefringence of the retinal nerve fiber layer. Invest Ophthalmol Vis Sci 2005;46:4588–93. [PubMed: 16303953]

25. Huang XR, Knighton RW, Cavuoto LN. Microtubule contribution to the reflectance of the retinal nerve fiber layer. Invest Ophthalmol Vis Sci 2006;47:5363–7. [PubMed: 17122125]

26. Fortune B, Wang L, Cull G, Cioffi GA. Intravitreal colchicine causes decreased RNFL birefringence without altering RNFL thickness. Invest Ophthalmol Vis Sci 2008;49:255–61. [PubMed: 18172100]

27. Anderson DR, Hendrickson A. Effect of intraocular pressure on rapid axoplasmic transport in monkey optic nerve. Invest Ophthalmol 1974;13:771–83. [PubMed: 4137635]

28. Quigley H, Anderson DR. The dynamics and location of axonal transport blockade by acute intraocular pressure elevation in primate optic nerve. Invest Ophthalmol 1976;15:606–16. [PubMed: 60300]

29. Minckler DS, Bunt AH, Klock IB. Radioautographic and cytochemical ultrastructural studies of axoplasmic transport in the monkey optic nerve head. Invest Ophthalmol Vis Sci 1978;17:33–50. [PubMed: 74368]

30. Quigley HA, Guy J, Anderson DR. Blockade of rapid axonal transport. Effect of intraocular pressure elevation in primate optic nerve. Arch Ophthalmol 1979;97:525–31. [PubMed: 84662]

31. Quigley HA, Addicks EM. Chronic experimental glaucoma in primates. II. Effect of extended intraocular pressure elevation on optic nerve head and axonal transport. Invest Ophthalmol Vis Sci 1980;19:137–52. [PubMed: 6153173]

32. Martin KR, Quigley HA, Valenta D, Kielczewski J, Pease ME. Optic nerve dynein motor protein distribution changes with intraocular pressure elevation in a rat model of glaucoma. Exp Eye Res 2006;83:255–62. [PubMed: 16546168]

33. Balaratnasingam C, Morgan WH, Bass L, Matich G, Cringle SJ, Yu DY. Axonal transport and cytoskeletal changes in the laminar regions after elevated intraocular pressure. Invest Ophthalmol Vis Sci 2007;48:3632–44. [PubMed: 17652733]

34. Balaratnasingam C, Morgan WH, Bass L, Cringle SJ, Yu DY. Time-dependent effects of elevated intraocular pressure on optic nerve head axonal transport and cytoskeleton proteins. Invest Ophthalmol Vis Sci 2008;49:986–99. [PubMed: 18326722]

35. Strouthidis NG, Yang H, Fortune B, Downs JC, Burgoyne CF. Detection of the Optic Nerve Head Neural Canal Opening within Three-Dimensional Histomorphometric and Spectral Domain Optical Coherence Tomography Data Sets. Invest Ophthalmol Vis Sci. 2008

36. Choplin NT, Zhou Q, Knighton RW. Effect of individualized compensation for anterior segment birefringence on retinal nerve fiber layer assessments as determined by scanning laser polarimetry. Ophthalmology 2003;110:719–25. [PubMed: 12689893]

37. RNFL Analysis with GDxVCC: A Primer and Clinical Guide. Laser Diagnostic Technologies, Inc.; San Diego, CA: 2004. GDxVCC-Instrument-manual.

38. Qiao-Grider Y, Hung LF, Kee CS, Ramamirtham R, Smith EL 3rd. A comparison of refractive development between two subspecies of infant rhesus monkeys (Macaca mulatta). Vision Res 2007;47:1668–81. [PubMed: 17442365]

39. Heickell AG, Bellezza AJ, Thompson HW, Burgoyne CF. Optic disc surface compliance testing using confocal scanning laser tomography in the normal monkey eye. J Glaucoma 2001;10:369–82. [PubMed: 11711833]

40. Fortune B, Cull GA, Burgoyne CF. Relative course of retinal nerve fiber layer birefringence and thickness and retinal function changes after optic nerve transection. Invest Ophthalmol Vis Sci 2008;49:4444–52. [PubMed: 18566463]

41. Hood DC, Fortune B, Arthur SN, Xing D, Salant JA, Ritch R, Liebmann JM. Blood vessel contributions to retinal nerve fiber layer thickness profiles measured with optical coherence tomography. J Glaucoma 2008;17:519–28. [PubMed: 18854727]

42. Coleman AL, Quigley HA, Vitale S, Dunkelberger G. Displacement of the optic nerve head by acute changes in intraocular pressure in monkey eyes. Ophthalmology 1991;98:35–40. [PubMed: 2023730]

43. Burgoyne CF, Varma R, Quigley HA, Vitale S, Pease ME, Lenane PL. Global and regional detection of induced optic disc change by digitized image analysis. Arch Ophthalmol 1994;112:261–8. [PubMed: 8311780]

44. Burgoyne CF, Quigley HA, Thompson HW, Vitale S, Varma R. Measurement of optic disc compliance by digitized image analysis in the normal monkey eye. Ophthalmology 1995;102:1790–9. [PubMed: 9098279]

45. Piette S, Liebmann JM, Ishikawa H, Gurses-Ozden R, Buxton D, Ritch R. Acute conformational changes in the optic nerve head with rapid intraocular pressure elevation: implications for LASIK surgery. Ophthalmic Surg Lasers Imaging 2003;34:334–41. [PubMed: 12875468]

46. Meredith SP, Swift L, Eke T, Broadway DC. The acute morphologic changes that occur at the optic nerve head induced by medical reduction of intraocular pressure. J Glaucoma 2007;16:556–61. [PubMed: 17873718]

47. Aydin A, Wollstein G, Price LL, Fujimoto JG, Schuman JS. Optical coherence tomography assessment of retinal nerve fiber layer thickness changes after glaucoma surgery. Ophthalmology 2003;110:1506–11. [PubMed: 12917164]

48. Rebolleda G, Munoz-Negrete FJ, Noval S. Evaluation of changes in peripapillary nerve fiber layer thickness after deep sclerectomy with optical coherence tomography. Ophthalmology 2007;114:488–93. [PubMed: 17123609]

49. Chang PT, Sekhon N, Budenz DL, Feuer WJ, Park PW, Anderson DR. Effect of lowering intraocular pressure on optical coherence tomography measurement of peripapillary retinal nerve fiber layer thickness. Ophthalmology 2007;114:2252–8. [PubMed: 17466378]

50. Iester M, Tizte P, Mermoud A. Retinal nerve fiber layer thickness changes after an acute increase in intraocular pressure. J Cataract Refract Surg 2002;28:2117–22. [PubMed: 12498845]
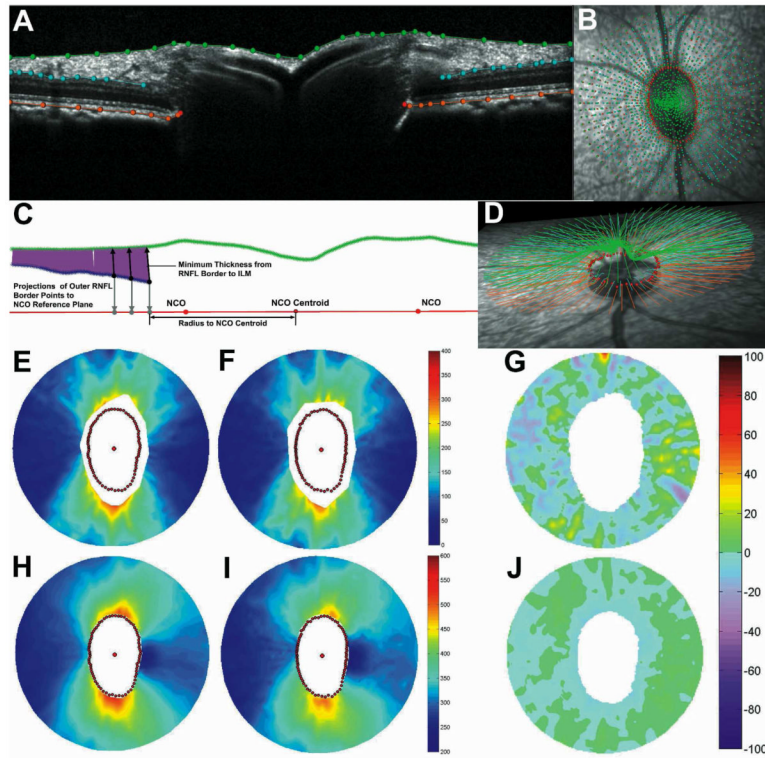
Figure 1.
Example of radial B-scan with results of manual segmentation (**A**, see text for details). Manual segmentation marks overlaid onto infrared fundus image (**B**). Schematic representation of method used to derive RNFL thickness values from segmentation results(**C**). Oblique view of full segmentation results for this eye (**D**). Topographic pseudo-color maps representing RNFL thickness (**E** and **F**) and total retinal thickness (**H** and **I**) after 30 min of IOP set to 10 mmHg (E and H), and after 60 min of IOP set to 45 mmHg (F and I). Topographic map representing % change of RNFL thickness (**G**) and total retinal thickness (**J**) between baseline and elevated IOP timepoints.

Figure 2.
Horizontal B-scan sections through the center of the ONH of one eye. The B-scan in the top panel was acquired after 30 min of IOP set to 10 mmHg. The B-scan in the bottom panel was acquired after 60 min of IOP set to 45 mmHg. The dashed white reference line connects the furthest point on either side of the ONH at the posterior aspect of the RPE-BM complex. The ONH surface exhibited posterior displacement relative to the reference line when IOP was elevated to 45 mmHg for 60 min (arrowhead). Changes in the shape of the peripapillary connective tissues were also consistently observed, such as posterior bowing of the RPE-BM complex immediately adjacent to the ONH (arrows).
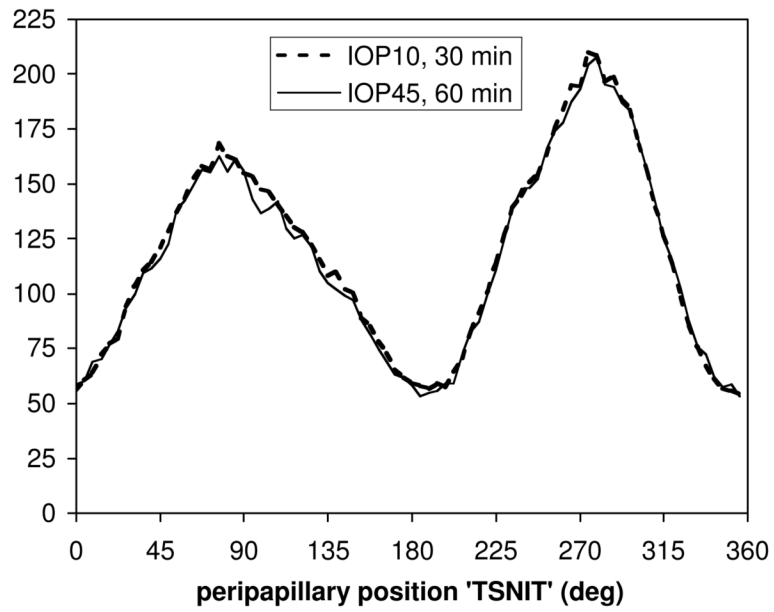
Figure 3.
Group average peripapillary RNFL thickness after 30 min of IOP set to 10 mmHg (bold dashed curve) and after 60 min of IOP set to 45 mmHg (thin solid curve).
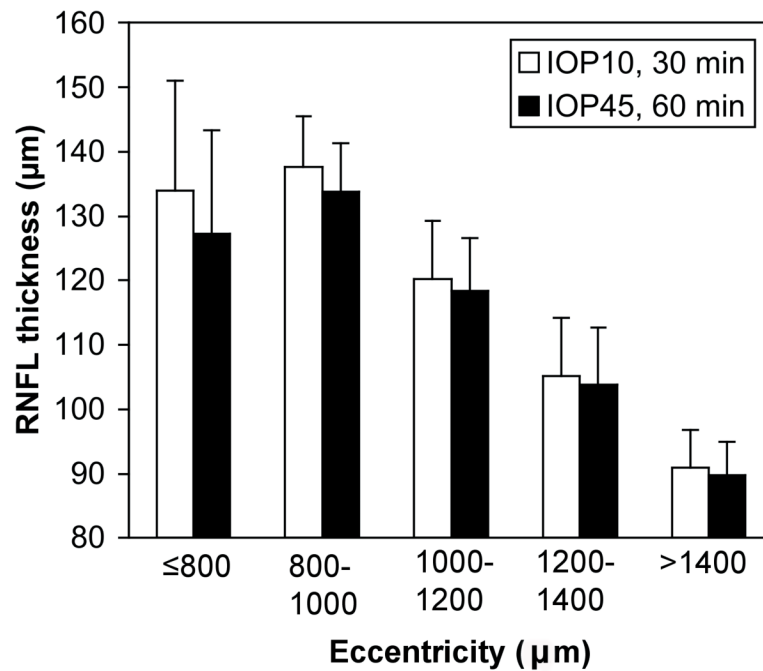
Figure 4.
Group average RNFL thickness versus eccentricity after 30 min of IOP set to 10 mmHg (open bars) and after 60 min of IOP set to 45 mmHg (filled bars). Error bars represent standard deviation (10 eyes, 5 animals). Note that eccentricity values represent the linear dimension converted from angular subtense by the Spectralis instrument then scaled 0.8x for the NHP eye assuming a 19 mm axial length.
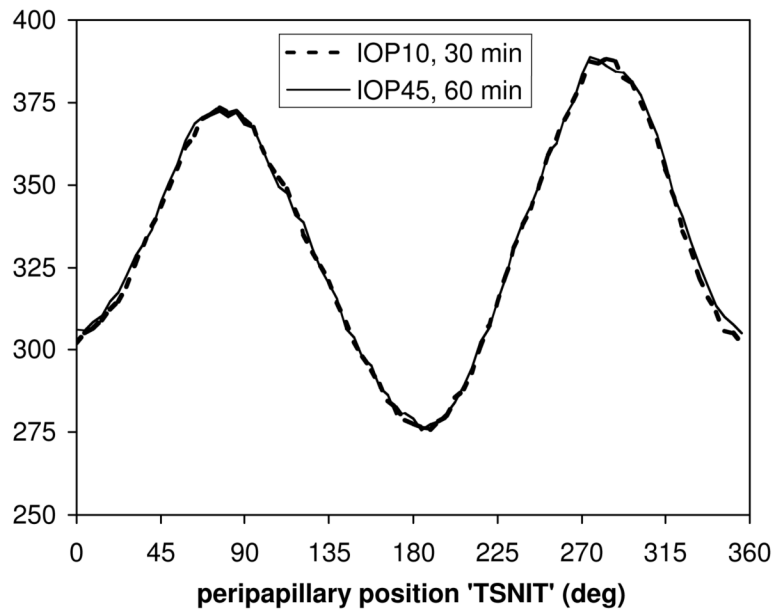
Figure 5.
Group average peripapillary retinal thickness after 30 min of IOP set to 10 mmHg (bold dashed curve) and after 60 min of IOP set to 45 mmHg (thin solid curve).
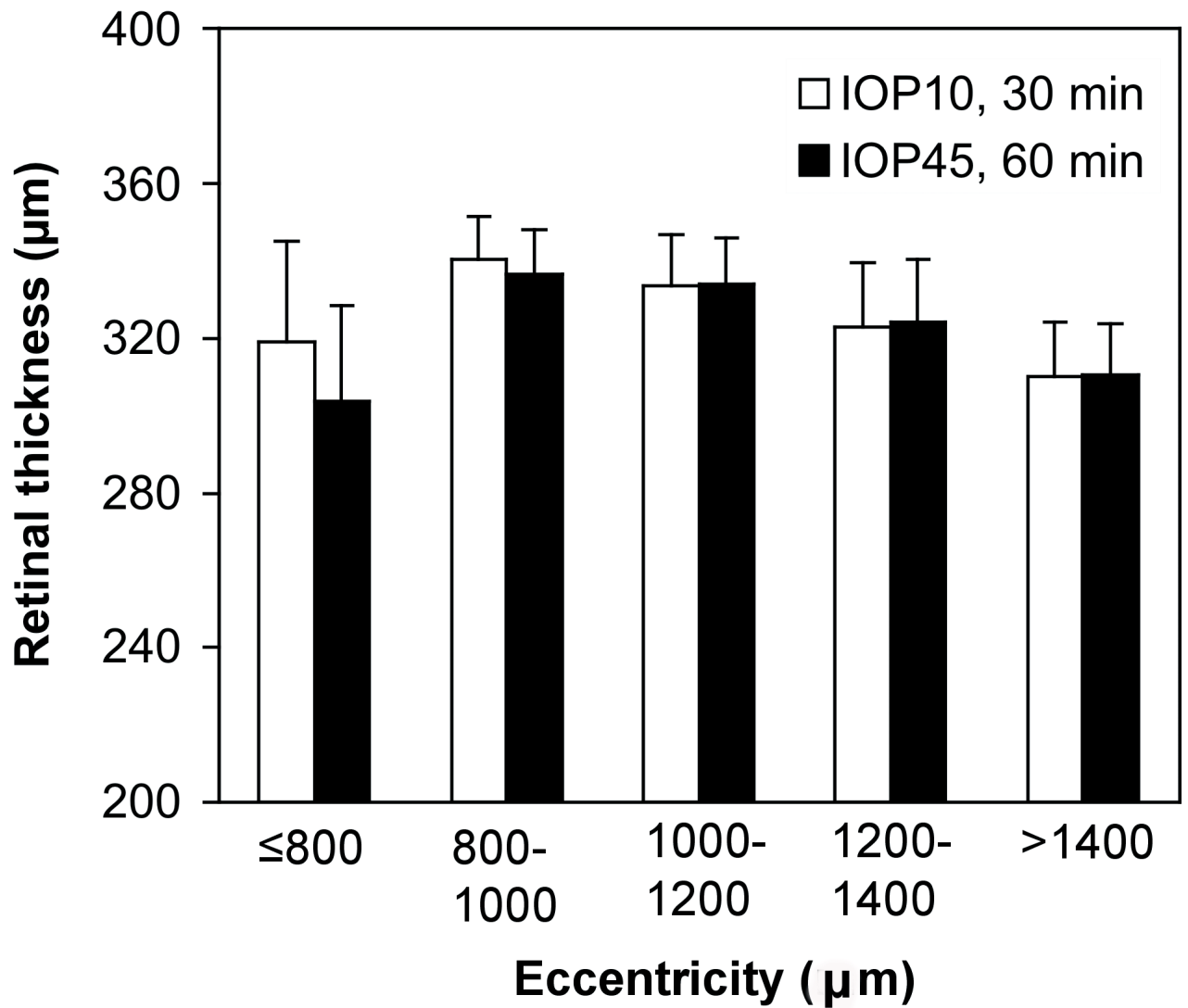
Figure 6.
Group average retinal thickness versus eccentricity after 30 min of IOP set to 10 mmHg (open bars) and after 60 min of IOP set to 45 mmHg (filled bars). Error bars represent standard deviation (10 eyes, 5 animals).
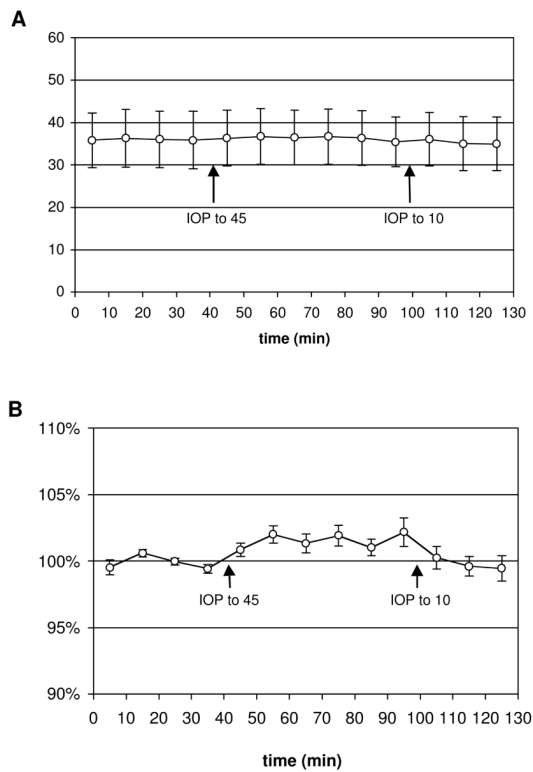
Figure 7.
Group average peripapillary RNFL retardance (± SD; n=8 eyes, 4 monkeys) versus time (**A**). Retardance values for each eye are normalized to their average baseline value and plotted (±SEM) versus time in the lower panel (**B**). Arrows indicate when IOP was elevated from baseline (IOP =10 mmHg) to IOP = 45 mmHg, and when IOP was lowered back to IOP = 10 mmHg.

Table 1

Age, weight, and experimental group assignment for each animal in this study. Number in parentheses after OCT indicates the number of radial B-scans acquired during the experiment

Animal	Age (years)	Weight (kg)	Experiment
1	13	5.2	SLP
2	12	5.8	SLP
3	10	6.4	SLP
4	12	6.6	SLP
5	10	4.0	OCT (80)
6	7	6.0	OCT (80)
7	8	7.2	OCT (80)
8	2	5.4	OCT (48)
9	1	2.7	OCT (48)